Synthesis, crystal structure and magnetic properties of A3A'RuO6 (A = Ca, Sr; A' = Li, Na)

Jacques Darriet, Fabien Grasset, Peter Battle

SYNTHESIS, CRYSTAL STRUCTURE AND MAGNETIC PROPERTIES OF $A_3A'RuO_6$ (A = Ca, Sr; A′ = Li, Na)

Jacques Darriet[1]*, Fabien Grasset[1] and Peter D. Battle[2]

[1]ICMCB, Château Brivazac, Av. Dr. Schweitzer, 33608 Pessac Cedex, France

[2] Inorganic Chemistry Laboratory, South Parks Road, Oxford OX1 3QR, UK

ABSTRACT The compounds $A_3A'RuO_6$ (A = Ca, Sr; A′ = Li, Na) have been synthesized by solid state reactions and studied by X-ray powder diffraction and magnetometry. They all adopt the K_4CdCl_6 (Sr_4PtO_6) structure with the cations A′ and Ru occupying the trigonal prismatic and octahedral sites respectively. Infinite chains of octahedra and trigonal prisms sharing faces run parallel to the *c* axis, the chains being separated by the cations A (Ca, Sr). The validity of this description of the structure is discussed in the light of magnetic susceptibility data which suggest that these phases all transform to a magnetically ordered state in the temperature range $70 < T/K < 120$. Preliminary results of powder neutron diffraction experiments confirm the presence of long-range magnetic order in the low temperature phase.

KEYWORDS: A. oxides C. neutron scattering, C. X-ray diffraction, C. magnetic properties, D. magnetic structure

INTRODUCTION

There has been a recent upsurge of interest in the solid state chemistry of ternary and quaternary oxides of the platinum metals. This has been driven largely by the observation that many of these compounds adopt crystal structures which apparently contain 1D chains of transition metal coordination polyhedra, thus introducing the possibility of unusual lectronic properties, but it has also been driven in part by recent progress in structural

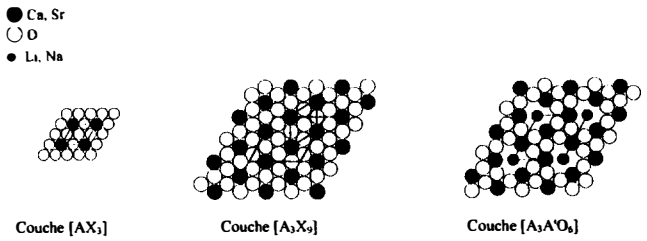

FIG. 1
Representation of the different layers.

chemistry, in particular the recognition that these structures are related to that of perovskite (1). The hexagonal perovskite structure is often thought of as a pseudo-*hcp* stack of AO_3 layers (A is usually an alkaline earth element) with transition metal cations B, occupying octahedral holes between the layers to give the stoichiometry ABO_3. This is sometimes conveniently referred to in terms of A_3O_9 layers, leading to the stoichiometry $A_3B_3O_9$. It has now been recognized that the structures of many oxides, the stoichiometry of which is not obviously related to that of perovskite, can be considered within the same structural framework if we allow for the inclusion of modified layer-types within the stacking sequence. For example, an ordered removal of three oxide ions from an A_3O_9 layer leads to the formation of an A_3O_6 layer, and the stacking sequence $(A_3O_6)_3(A_3O_9)$ leads to the overall stoichiometry A_4O_9. It has recently been shown (2) that this stacking sequence occurs in the crystal structure of $Sr_4Ru_2O_9$, with the Ru(V) cations occupying the octahedral sites which are formed between the layers. In addition to these octahedral sites, the hexagonal stacking of A_3O_6 layers leads to the creation of cation sites with trigonal prismatic coordination by oxygen. The creation of these sites, which lie within the A_3O_6 layers, is made possible by the reduced oxide concentration therein (Fig. 1). The trigonal prismatic sites are unoccupied in $Sr_4Ru_2O_9$. In compounds in which they are occupied, the stoichiometry of the layers is properly described as $A_3A'O_6$, where A and A′ may be the same element. The well-known K_4CdCl_6 structure (Fig. 2) can then be described as consisting of the stacking sequence $(A_3A'O_6)$, with (A = A′ = K) and with Cd occupying the octahedral sites between the layers. Many ternary oxides of Pt and Ir crystallize with this structure, for example Sr_4PtO_6 (3), Ca_4IrO_6 (4), Ca_4PtO_6 (5) Sr_4IrO_6 (6), and Ba_4PtO_6 (7). More recently, several quaternary

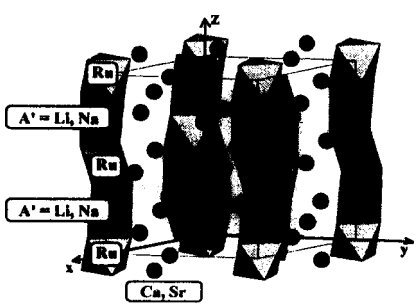

FIG. 2
Representation of the structure of $A_3A'RuO_6$ (A = Ca, Sr; A′ = Li, Na). (K_4CdCl_6-type structure.

TABLE 1
Cell Parameters of the $A_3A'RuO_6$ Compounds

Compounds	*a* (Å)	*c* (Å)	V (Å^3)
Ca_3LiRuO_6	9.2294(18)	10.7630(29)	793.98
Ca_3LiRuO_6 (200 K)	*9.2184(9)*	*10.7287(13)*	*789.56*
Ca_3NaRuO_6	9.2273(11)	11.1693(16)	823.58
Ca_3NaRuO_6 (150 K)	*9.2101(8)*	*11.1393(12)*	*818.32*
Sr_3LiRuO_6	9.6345(6)	11.1299(12)	894.72
Sr_3NaRuO_6	9.6192(10)	11.5271(19)	923.69

*The values printed in italic type correspond to neutron data.

members of this series have been reported, including Ca_3CuIrO_6 (8), $Ca_{3.5}Cu_{0.5}PtO_6$ (9), Sr_3MIrO_6 (M = Li, Na, Ca, Ni, Cu, Zn, Cd) (10–13), Sr_3MPtO_6 (M = Ni, Cu, Zn) (14–16), $Sr_3CuPt_{0.5}Ir_{0.5}O_6$ (17), Sr_3NiYbO_6 (18) and Ba_3NaIrO_6 (19). In the case of Ru, the only K_4CdCl_6-like compounds known to date are Sr_3NaRuO_6 (20) and Ba_3NaRuO_6 (19). "Ca_4RuO_6" has been reported in the literature (21) but our work shows clearly that the published chemical formula is wrong, and that the sample under consideration was actually

TABLE 2
Atomic Coordinates and Thermal Parameters in the $A_3A'RuO_6$ Compounds

Atom	Position	x	y	z	B(Å^2)
Ca	18e	0.3571(1)	0	–	1.51(4)
		0.3565(3)	*0*	–	*0.73(5)*
Li	6a	0	0	–	4.22(68)
		0	*0*	–	*2.57(27)*
Ru	6b	0	0	0	1.17(3)
		0	*0*	*0*	*0.44(6)*
O	36f	0.1824(4)	0.0281(4)	0.1039(3)	1.26(8)
		0.1835(2)	*0.0270(2)*	*0.1066(1)*	*0.84(4)*
Ca	18e	0.3567(2)	0	–	0.73(3)
		0.3558(2)	*0*	–	*0.54(5)*
Na	6a	0	0	–	0.92(9)
		0	*0*	–	*0.97(11)*
Ru	6b	0	0	0	0.51(2)
		0	*0*	*0*	*0.58(5)*
O	36f	0.1845(3)	0.0289(2)	0.1006(2)	0.48(6)
		0.1883(2)	*0.0301(2)*	*0.1002(1)*	*0.60(4)*
Sr	18e	0.3585(1)	0	–	0.49(1)
Li	6a	0	0	–	0.68(36)
Ru	6b	0	0	0	0.31(2)
O	36f	0.1767(3)	0.0233(3)	0.1055(2)	0.25(6)
Sr	18e	0.3580(6)	0	–	0.08(2)
Na	6a	0	0	–	0.05(9)
Ru	6b	0	0	0	0.07(2)
O	36f	0.1765(4)	0.0224(3)	0.1011(4)	0.13(6)

*The values printed in italic type correspond to neutron data.

TABLE 3
Main Interatomic Distances (Å) and R Factors in the $A_3A'RuO_6$ Compounds

Ca_3LiRuO_6		Ca_3NaRuO_6		Sr_3LiRuO_6		Sr_3NaRuO_6	
Li–O	2.222(3)	Na–O	2.302(3)	Li–O	2.2690(3)	Na–O	2.350(3)
Ru–O	1.928(3)	Ru–O	1.944(3)	Ru–O	1.986(3)	Ru–O	1.983(3)
Ca–O	2 × 2.356(4)	Ca–O	2 × 2.410(3)	Sr–O	2 × 2.469(3)	Sr–O	2 × 2.536(3)
	2 × 2.456(3)		2 × 2.453(3)		2 × 2.580(2)		2 × 2.604(3)
	2 × 2.465(3)		2 × 2.485(3)		2 × 2.610(2)		2 × 2.610(3)
	2 × 2.710(3)		2 × 2.716(4)		2 × 2.781(3)		2 × 2.770(4)
R_I = 5.69%		R_I = 5.26%		R_I = 2.66%		R_I = 3.19%	
R_I = 5.79%		*R_I = 7.21%*		R_p = 8.10%		R_p = 8.95%	
R_p = 11.7%		R_p = 7.63%		R_{wp} = 11.7%		R_{wp} = 12.0%	
R_p = 8.92%		*R_p = 6.72%*					
R_{wp} = 15.9%		R_{wp} = 10.2%					
R_{wp} = 11.8%		*R_{wp} = 8.64%*					

*The values printed in italic type correspond to neutron data.

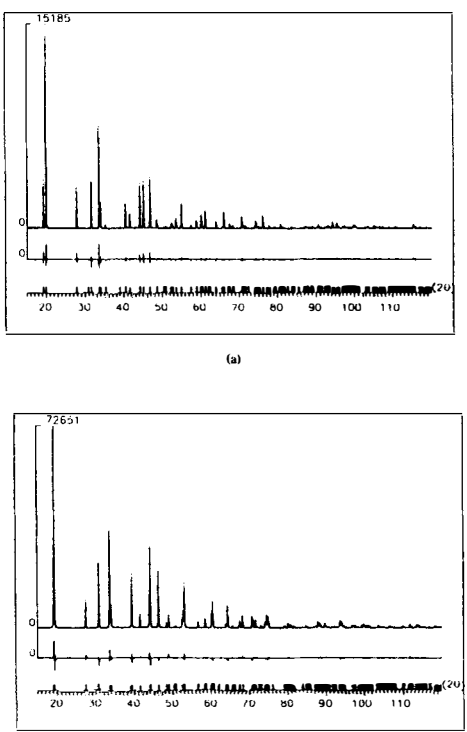

FIG. 3
Observed (dots), calculated (full line), and difference X-ray powder diffraction profiles of Ca_3LiRuO_6 (a) and Ca_3NaRuO_6 (b).

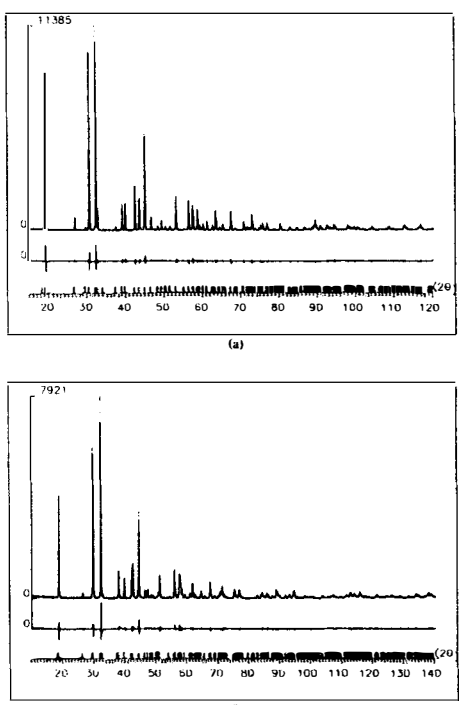

FIG. 4
Observed (dots), calculated (full line), and difference X-ray powder diffraction profiles of Sr_3LiRuO_6 (a) and Sr_3NaRuO_6 (b).

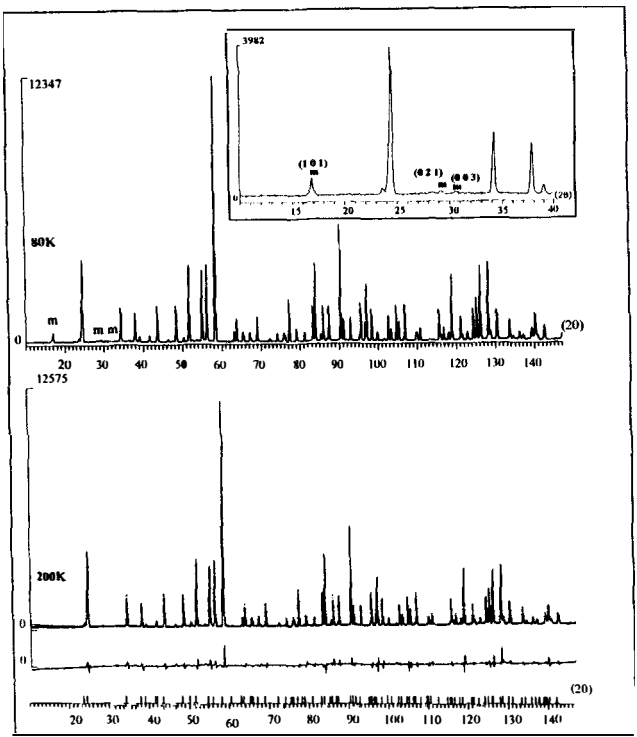

FIG. 5

Observed (T = 80 K) and observed and calculated (T = 200 K) neutron powder diffraction of Ca_3LiRuO_6. Magnetic peaks are marked by m.

Ca_3NaRuO_6. We have now synthesized the family of compounds $A_3A'RuO_6$ (A = Ca, Sr; A′ = Li, Na) and the present paper gives an account of the structural chemistry and magnetic properties of the new compounds Ca_3LiRuO_6, Ca_3NaRuO_6, and Sr_3LiRuO_6. The magnetic properties of Sr_3NaRuO_6, which was originally isolated by Frenzen and Müller-Buschbaum (20), are included for completeness. There is some debate as to whether the magnetic properties of these materials can reasonably be treated using a 1D model (11,22) and we present below the preliminary results of neutron diffraction experiments which may resolve this point.

EXPERIMENTAL

Sample Preparations. $CaRuO_3$ and $SrRuO_3$ were prepared by the equimolar reaction of $CaCO_3$ (Aldrich 99.9%) or $SrCO_3$ (Aldrich 99.5%) and RuO_2 (Aldrich 99.99%) heated in air at 750°C for 24 hrs and then for 8 days at 1100°C and 1200°C, respectively. Polycrystalline samples of $A_3A'RuO_6$ (A = Ca, Sr; A′ = Li, Na) were then prepared via solid state reactions between the corresponding $ARuO_3$ (A = Ca, Sr), $SrCO_3$, $CaCO_3$, Li_2CO_3 (Strem Chemical 99.99%), and Na_2CO_3 (Strem Chemical 99.5%). The initial mixture was mixed in an agate mortar and heated in a gold crucible at 550°C for 24 hrs to decompose the carbonates. Subsequently, the powders were ground and heated at 800°C for 24 hrs and at 950°C for two weeks with intermediate grindings. All the preparations were carried out under a flow of

oxygen. After the final heating, the powders were cooled slowly down to room temperature. The progress of the reactions was monitored using X-ray powder diffraction (XRD), and they were deemed to be complete when the diffraction pattern did not change on heating the sample further.

The Sr compounds (but not the Ca analogues) are unstable in air, decomposing after exposure for one week.

Structural Characterization. Powder X-ray diffraction data were recorded at room temperature on a Philips X'pert MPD using Bragg-Brentano geometry with CuKa radiation. Step scans were performed over the angular range $15 < 2\theta/° < 120$ for Ca_3LiRuO_6, Ca_3NaRuO_6, and Sr_3LiRuO_6, and $10 < 2\theta/° < 140$ for Sr_3NaRuO_6; a 2θ step size of 0.02° was used in all cases. Rietveld refinements (23) were performed using the Fullprof program package (24). The peak shape was described by a pseudo-Voigt function and the background level was defined by a polynomial function with six refinable coefficients. For each diffraction pattern, a scale factor, a counter zero point, and the unit-cell parameters were refined in addition to the atomic parameters.

The high-resolution diffractometer at beam line H1A of the high-flux beam reactor at Brookhaven National Laboratory was used to collect neutron powder diffraction data on Ca_3LiRuO_6 and Ca_3NaRuO_6 at a wavelength of 1.8857 Å over the angular range $10 < 2\theta/° < 150$, using a 2θ step size of 0.05°. Data were collected at 200 and 80 K on Ca_3LiRuO_6 and at 150 and 20 K on Ca_3NaRuO_6.

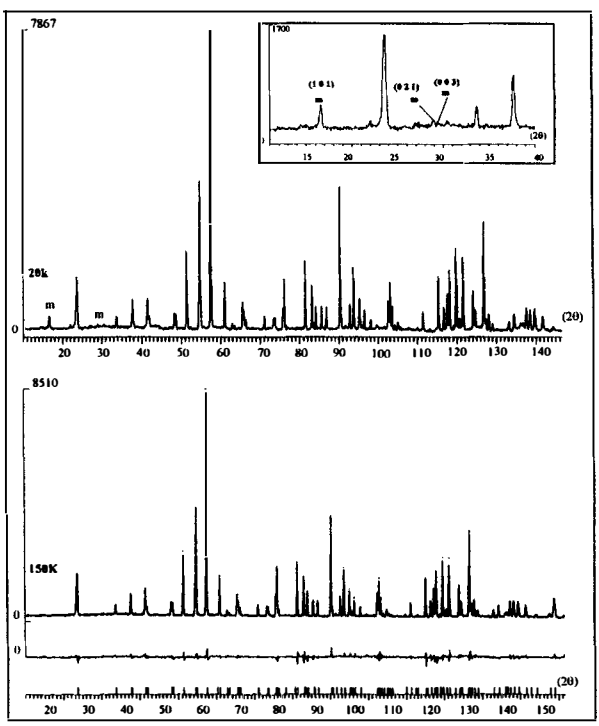

FIG. 6

Observed (T = 20 K) and observed and calculated (T = 150 K) neutron powder diffraction of Ca_3NaRuO_6. Magnetic peaks are marked by m.

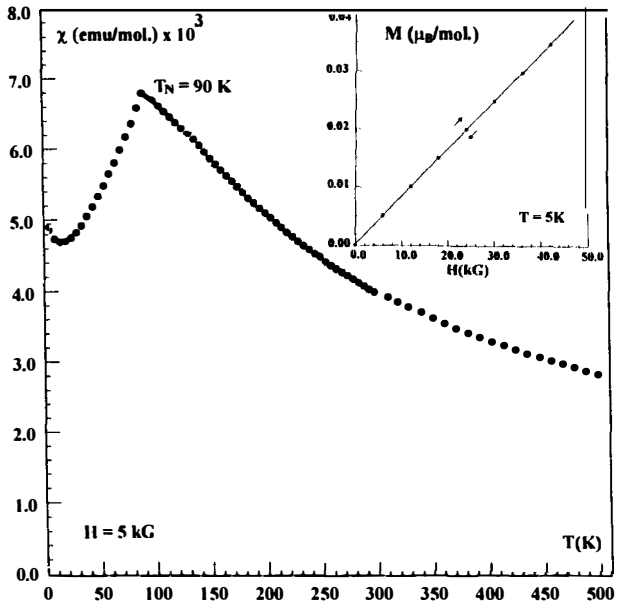

FIG. 7

Experimental thermal variation of the susceptibility of Ca_3NaRuO_6 at H = 5 kG. The variation of the magnetization with H at T = 5 K is represented in the inset.

Magnetic Measurements. Magnetic susceptibilities were measured using a Quantum Design superconducting quantum interference device (SQUID) magnetometer. Measurements were taken in different applied fields up to 5T in the temperature range $2 < T/K < 300$ after cooling the sample in zero magnetic field (zero-field cooled, ZFC) and also after cooling in the measuring field (field cooled, FC). Measurements in the temperature range $300 < T/K < 500$ were carried out using a MANICS susceptometer. No correction was made for the diamagnetic contributions of the different cations.

RESULTS

Analysis of our X-ray powder diffraction data indicates that the members of the $A_3A'RuO_6$ series (A = Ca, Sr; A′ = Li, Na) are isostructural with rhombohedral K_4CdCl_6 (25) and Sr_4PtO_6 (3). The lattice parameters refined from the X-ray powder patterns (using silicon as a standard) are given in Table 1. The unit-cell parameters of Ca_3NaRuO_6 are very close to

TABLE 4
Magnetic Parameters of the $A_3A'RuO_6$ Compounds

	Ca_3LiRuO_6	Ca_3NaRuO_6	Sr_3LiRuO_6	Sr_3NaRuO_6
C (emu·K/mol)	2.11(2)	1.90(1)	1.94(1)	1.89(1)
θ_p (K)	−261(2)	−171(2)	−165(2)	−124(2)
μ_{eff} (μ_B)	3.00 at 300 K	3.36 at 500 K	3.14 at 300 K	3.30 at 300 K
T_N (K)	120(2)	90(2)	90(2)	70(2)

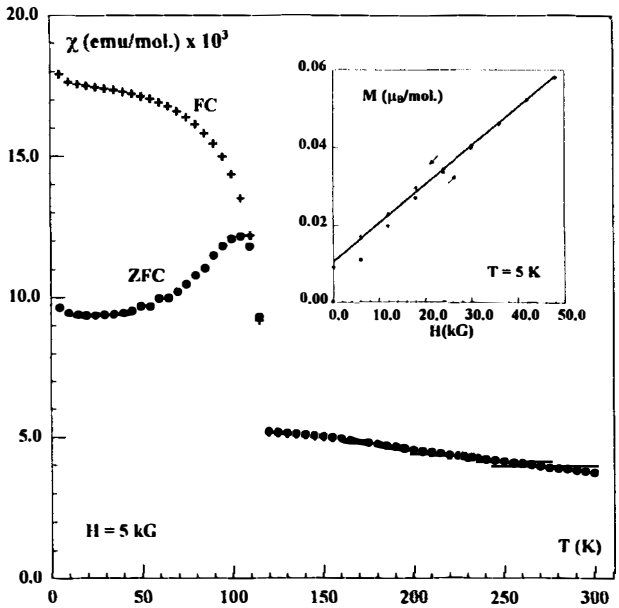

FIG. 8

Experimental thermal variation of the susceptibility of Ca_3LiRuO_6 at H = 5 kG. ● Zero-field cooled; + Field cooled. The variation of the magnetization with H at T = 5 K is represented in the inset.

those reported previously for "Ca_4RuO_6" (21) (a = 9.25 Å, c = 11.17 Å). The earlier preparation was carried out from a mixture of Ru, Na_2CO_3, and $CaCO_3$, and it is thus easy to understand the misassignment of the composition. Our attempts to prepare Ca_4RuO_6 from a stoichiometric mixture of RuO_2 and CaO at various temperatures up to 1000 °C under a flow of inert gas or oxygen were unsuccessful.

The structural refinements were carried out in the space group $R\bar{3}c$ (no. 167), using the structure of Sr_4PtO_6 (3) as a starting model. The ruthenium atom (Ru^{5+}) replaces the platinum (Pt^{4+}) in the 6b position and the lithium or sodium atoms occupy the 6a position (A′) which is occupied by Sr in Sr_4PtO_6. The refined atomic positions and isotropic thermal parameters are listed in Table 2. The results obtained for Sr_3NaRuO_6 are in very good agreement with those reported previously (20). The final R values and the principal interatomic distances are given in Table 3. The observed, calculated, and difference X-ray diffraction profiles are shown in Figures 3 and 4.

The values of the Li–O distances, 2.222 Å (Ca_3LiRuO_6) and 2.269 Å (Sr_3LiRuO_6), and Na–O distances, 2.302 Å (Ca_3NaRuO_6) and 2.350 Å (Sr_3NaRuO_6), are similar to those found in the literature (26), although the refinement program almost certainly overestimates the precision with which these bond lengths can be measured in an X-ray powder diffraction experiment. The Ru^{V}–O bond distances (1.928 Å < d < 1.986 Å) are in good agreement with those found in analogous compounds of pentavalent Ru (27).

The structures of Ca_3LiRuO_6 (T = 200 K) and Ca_3NaRuO_6 (T = 150 K) were also refined by Rietveld analysis of neutron powder diffraction data. The results agree very well with those obtained using X-rays (Tables 1, 2, and 3; Figs. 5 and 6). Additional peaks are observed in the diffraction patterns recorded at lower temperatures, for example: T = 20 K

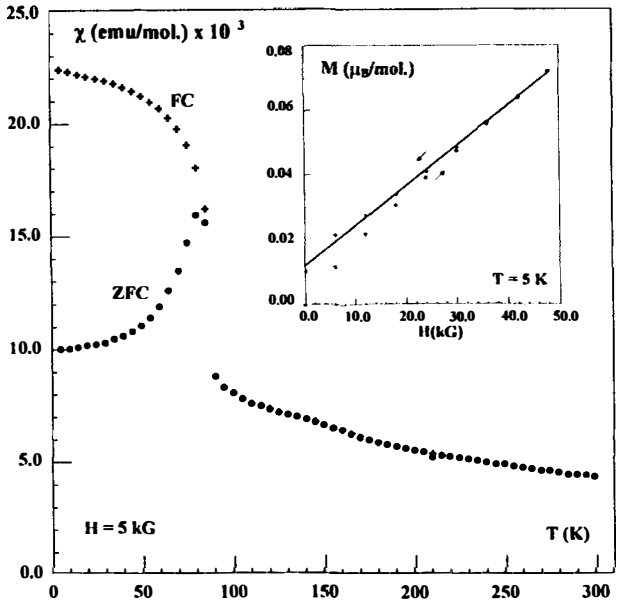

FIG. 9

Experimental thermal variation of the susceptibility of Sr_3LiRuO_6 at H = 5 kG. ● Zero-field cooled; + Field cooled. The variation of the magnetization with H at T = 5 K is represented in the inset.

for Ca_3NaRuO_6 and T = 80 K for Ca_3LiRuO_6 (Figs. 5 and 6). They can be indexed without changing the unit cell size, and correspond to the {101}, {021} and {003} reflections (Figs. 5 and 6). Their presence suggests the onset of long-range magnetic ordering, and the adoption of a magnetic structure which lacks the glide plane present in the crystal structure. The intensity of these magnetic peaks is, in both cases, too weak to allow a full determination of the magnetic structure, but the observation of $\{003\}_m$ proves that the ordered spins do not lie along the crystallographic *z* axis.

The ZFC and FC magnetic susceptibilities of Ca_3NaRuO_6 overlie at all temperatures and show a maximum at 90 K, thus suggesting that this compound shows long-range antiferromagnetic order at low (<90 K) temperatures (Fig. 7). This conclusion is consistent with the neutron diffraction data described above, and also with the negative value of θ (Table 4) obtained by fitting the high temperature portion of the susceptibility data to a Curie-Weiss law. The fitted Curie constant, C, is close to the localized electron, spin-only value (1.88 emu·K/mol) expected for a Ru^{5+}:$4d^3$ cation on an octahedral site. The Curie-Weiss parameters (C, θ) of Ca_3LiRuO_6, Ca_3NaRuO_6, and Sr_3NaRuO_6 are also characteristic of antiferromagnetically interacting Ru^{5+} cations, but the divergence of the ZFC and FC susceptibilities (Figs. 8, 9, and 10) and the observation of a remanent magnetization (0.01 to 0.02 μ_B/mol) at 5K (inset, Figs. 8, 9, and 10) suggest that the magnetic phase transition in these samples is from a paramagnet to a weak ferromagnet, that is a canted antiferromagnet; no remanent magnetization was observed in the case of Ca_3NaRuO_6 (inset, Fig. 7). The temperature at which the remanent magnetization of the three weak ferromagnets decreased to zero (Fig. 11) corresponds to the temperature of the maximum in the ZFC susceptibility and can be identified as the critical temperature, T_c. As in the case of Ca_3NaRuO_6, this

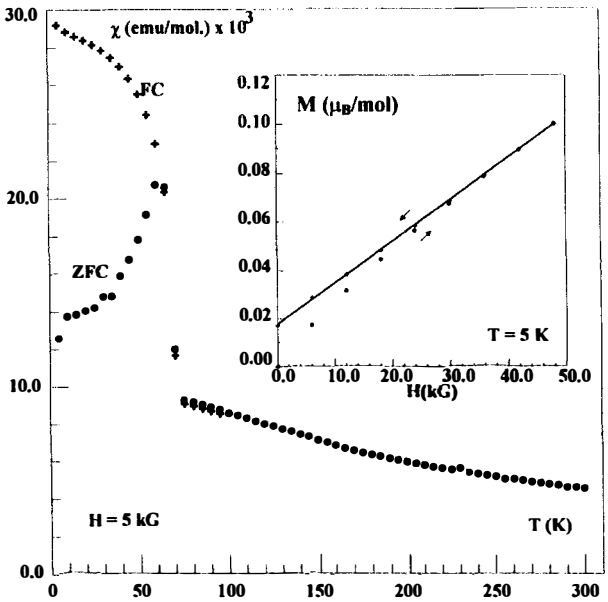

FIG. 10

Experimental thermal variation of the susceptibility of Sr_3NaRuO_6 at H = 5 kG. ● Zero-field cooled; + Field cooled. The variation of the magnetization with H at T = 5 K is represented in the inset.

interpretation of the magnetic susceptibility data is consistent with the neutron diffraction data described above.

DISCUSSION

It has been shown above that the $A_3A'RuO_6$ series (A = Ca, Sr; A′ = Li, Na) is isostructural with Sr_4PtO_6. The structure can be considered to consist of ($Ru/A'O_6$) chains (A′ = Li, Na) which are parallel to the *c* axis and which are separated from each other by the calcium or strontium atoms which maintain charge balance (Fig. 1). Within the chains, (RuO_6) octahedra are linked by common faces to the trigonal prisms, which are occupied by lithium or sodium atoms. Certain aspects of the structure can usefully be considered in terms of the A_3O_9 and $A_3A'O_6$ layers referred to above. The replacement of three oxygen atoms in a close packed [A_3O_9] layer by only one A′ atom (A′ = Li, Na) in the [$A_3A'O_6$] layer results in a decrease in the compactness of the layer. The consequence of this is a decrease in the coordination number of the A cations (A = Ca, Sr) from twelve in the case of a perovskite, where only A_3O_9 layers are present, to eight in the case of the $A_3A'RuO_6$ series, where only layers of composition [$A_3A'O_6$] are present. The two different environments are compared in Figure 12; in moving from A_3O_9 to $A_3A'O_6$, two adjacent oxygen atoms are removed from the central layer, and also one from each of the two adjacent layers.

The thermal variation of the magnetic susceptibilities of the $A_3A'RuO_6$ compounds considered in this study is characteristic of compounds which show 3-dimensional long-range magnetic order. The ordering temperatures range between 70 and 120 K (Table 4) and

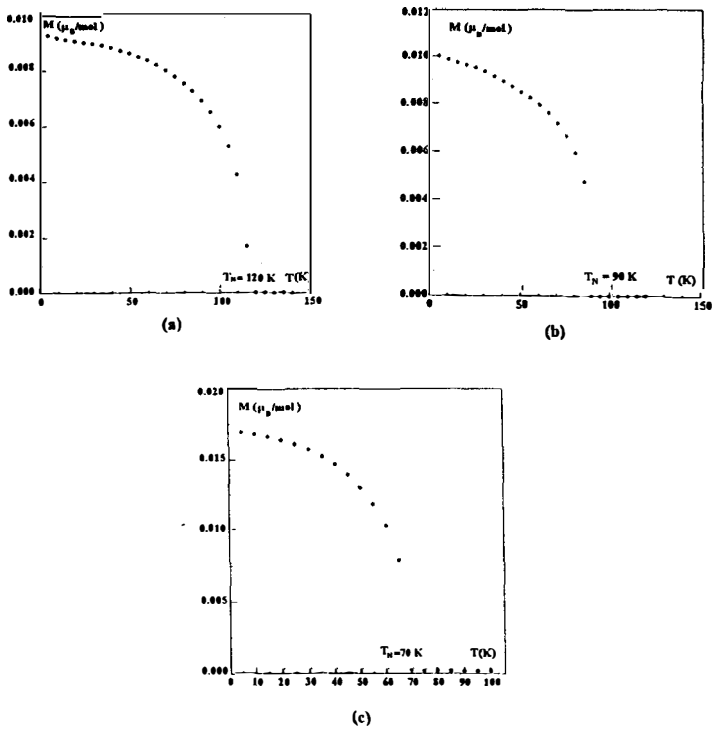

FIG. 11

Thermal dependence of the remanent magnetization of Ca_3LiRuO_6 (a) Sr_3LiRuO_6 (b), and Sr_3NaRuO_6 (c).

are thus high compared to analogous compounds of Ir and Rh (12,22). This observation might be explained by the electronic configuration of Ru^V (d^3) in octahedral symmetry where there is no first-order orbital contribution to the magnetic moment. For a given atom A (A = Ca, or Sr), the ordering temperature increases as the size of the A′ atom (Li, Na) decreases. This composition-dependence of the critical temperature is consistent with a

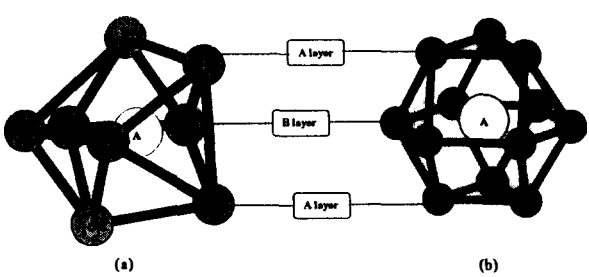

FIG. 12

Representation of the environments of the cation A in the $A_3A'RuO_6$ compounds (A = Ca, Sr; A′ = Li, Na) (a) and in the 2H hexagonal perovskite (b).

strengthening of the magnetic interactions as the unit-cell volume decreases and the superexchange pathways get shorter. We do not presently have an explanation for the difference in behavior of Ca_3NaRuO_6 (antiferromagnetic) and the other three (weakly ferromagnetic) compounds. It is unfortunate that the counting statistics obtained in the neutron diffraction experiments performed to date do not allow a reliable refinement of the magnetic structure. We shall pursue this point in the near future. However, the mere observation of magnetic Bragg peaks at a temperature of 80 K confirms that 3-dimensional long-range magnetic order is present. Nguyen et al. (11,16,17) have described a series of isostructural compounds containing Ir or Pt. They modeled their magnetic susceptibility data by assuming that this crystal structure can be thought of as 1-dimensional. The observation of long-range magnetic ordering above 100 K throws serious doubt on such a model. Moreover the intra- and interchain Ru–Ru distances are very similar (5.756 Å and 5.875 Å in Sr_3NaRuO_6), and we believe that neither the structural nor the magnetic data support the description of the structure as 1-dimensional.

REFERENCES

1. J. Darriet and M. A. Subramanian, *J. Mater. Chem.* 5, 543 (1995).
2. C. Dussarrat, J. Fompeyrine and J. Darriet, *Eur. J. Solid State Chem.* 32, 3 (1995).
3. J. R. Randall and L. Katz, *Acta Crystallogr.* 12, 519 (1959).
4. R.F. Sarkozy, C.W. Moeller and B.L. Chamberland, *J. Solid State Chem.* 9, 242 (1974).
5. I.S. Shaplygin and V.B. Lazarev, *Mater. Res. Bull.* 10, 903 (1975).
6. A.V. Powell, P.D. Battle and J.G. Gore, *Acta Crystallogr. C* 49, 189 (1993).
7. A.P. Wilkinson and A.K. Cheetham, *Acta Crystallogr. C* 45, 1672 (1989).
8. A. Tomaszewska and H. Müller-Buschbaum, *Z. Anorg. Allg. Chemie.* 619, 534 (1993).
9. A. Tomaszewska and H. Müller-Buschbaum, *Z. Anorg. Allg. Chemie* 617, 23 (1992).
10. S. Frenzen and H. Müller-Buschbaum, *Z. Naturforsch.* 51b, 225 (1996).
11. T.N. Nguyen and H.C. zur-Loye, *J. Solid State Chem.* 117, 300 (1995).
12. N. Segal, J.F. Vente, T.S. Bush and P.D. Battle, *J. Mater. Chem.* 6, 395 (1996).
13. M. Neubacher and H. Müller-Buschbaum, *Z. Anorg. Allg. Chemie* 607, 124 (1992).
14. C. Lampe-Önnerud and H.C. ZurLoye, *Inorg. Chem.* 35, 2155 (1996).
15. A.P. Wilkinson, A.K. Cheetham, W. Kunnman and A. Kvick, *Eur. J. Solid State Chem.* 28, 453 (1991).
16. T.N. Nguyen, D.M. Giaquinta and H.C. zur-Loye, *Chem. Mater.* 6, 1642 (1994).
17. T.N. Nguyen, P.A. Lee and H.-C. zur-Loye, *Science* 271, 489 (1996).
18. M. James and J.P. Attfield, *J. Mater. Chem.* 4, 575 (1994).
19. S. Frenzen and H. Müller-Buschbaum, *Z. Naturforsch.* 51b, 1204 (1996).
20. S. Frenzen and H. Müller-Buschbaum, *Z. Naturforsch.* 50b, 581 (1995).
21. W.D. Komer and D.J. Machin, *J. Less-Common Met.* 61, 91 (1978).
22. J.F. Vente, J.K. Lear and P.D. Battle, *J. Mater. Chem.* 5, 1785 (1995).
23. H.M. Rietveld, *J. Appl. Crystallogr.* 2, 65 (1969).
24. J. Rodriguez-Caravajal, *FULLPROF*, (1995): LLB Saclay, France.
25. G. Bergerhoff and O. Schimtz-Dumont, *Z. Anorg. Allg. Chem.* 284, 10 (1956).
26. P.D. Battle and S.H. Kim, *J. Solid State Chem.* 101, 161 (1992).
27. P.D. Battle and W.J. Macklin, *J. Solid State Chem.* 52, 138 (1984).